MEMO 10-9-58E

NASA MEMO 10-9-58E

NASA

MEMORANDUM

HEAT-TRANSFER AND FRICTION MEASUREMENTS WITH VARIABLE PROPERTIES FOR AIRFLOW NORMAL TO FINNED AND UNFINNED TUBE BANKS

By Robert G. Ragsdale

Lewis Research Center
Cleveland, Ohio

NATIONAL AERONAUTICS AND SPACE ADMINISTRATION
WASHINGTON
December 1958

TABLE OF CONTENTS

NATIONAL AERONAUTICS AND SPACE ADMINISTRATION

NASA MEMO 10-9-58E

HEAT-TRANSFER AND FRICTION MEASUREMENTS WITH VARIABLE PROPERTIES FOR AIRFLOW NORMAL TO FINNED AND UNFINNED TUBE BANKS

By Robert G. Ragsdale

4880

SUMMARY

A single-line correlation of both the heat-transfer and pressure-drop data for electrically heated unfinned tubes is obtained by evaluating the density in the Reynolds number, specific heat, thermal conductivity, and viscosity at the film temperature, and the density in the friction coefficient at the bulk temperature.

The heat-transfer data for finned tubes also exhibit an effect of physical-property variation which is removed by evaluating all properties, including density, at the primary surface temperature, and using $k^* = 0.015\sqrt{T/530}$ for the thermal conductivity of air where T is the absolute temperature. The pressure drop for finned tubes is correlated by the use of bulk density in both the Reynolds number and friction coefficient.

The data reported are for Reynolds numbers from 2000 to 35,000, surface temperatures from 600° to 1400° R, and an air inlet temperature of 530° R.

CH-1

INTRODUCTION

The performance characteristics of a given heat-exchange system are normally represented by fluid parameters which describe physical properties, velocity, and a basic dimension such as diameter. In systems of relatively small temperature differences, physical properties are reasonably constant. They can be evaluated at an average fluid temperature; however, large temperature differences may result in sufficient variation of physical properties so that this procedure is inadequate. The effect of physical-property variation on heat transfer to fluids in turbulent motion is extremely difficult to predict. Previous experimental results (ref. 1) for heat transfer to air flowing through round smooth tubes

indicate an effect of surface-to-bulk temperature ratio. Reference 1 successfully correlates the data by evaluating the fluid density at a film temperature. A theoretical treatment of this problem is given in reference 2.

As a part of a general program of high-temperature heat-transfer research at Lewis laboratory, an experimental investigation was made of the average heat-transfer and pressure-drop characteristics of two basic heat-exchanger core types, airflow normal to staggered banks of both finned and unfinned tubes. Data published for these configurations (refs. 3 to 6) are for relatively low-temperature differences and heat fluxes. This report extends the experimental study of physical-property variation to include flow normal to banks of both finned and unfinned tubes.

SYMBOLS

A minumum cross-sectional flow area

c_p specific heat

d diameter

f friction factor

G mass velocity, w/A

g_c gravitational constant

h average air film heat-transfer coefficient

k thermal conductivity

k* $0.015\sqrt{T/530}$

L exchanger length

l fin height

m fin parameter, $\sqrt{2h/k_f\delta}$

Nu Nusselt number, (hd/k)

Pr Prandtl number, $(c_p\mu/k)$

p static pressure

Q heat-flow rate

Re	Reynolds number, $(dV\rho/\mu)$
S	total heat-transfer surface area
T	absolute temperature, ^{o}R
V	bulk velocity, $(w/\rho_b A)$
w	weight-flow rate
Δ	difference
δ	fin thickness, ft
η	efficiency
μ	viscosity
ρ	density

Subscripts:

a	local bulk
av	average
b	bulk
f	film
f	fin or friction
H	hydraulic
m	mean
o	over-all
s	primary surface
t	tube
1	inlet
2	outlet

EXPERIMENTAL APPARATUS

Over-All Setup

Figure 1 is a schematic representation of the experimental apparatus. Air was delivered at 40 pounds per square inch gage through an ASME standard flange-type orifice run in a 4-inch-diameter pipe. An enlarged section served both as a filter housing and plenum chamber. The air then passed through a flow control valve and into a transition section. The transition section altered the flow passage from a 3-inch-diameter circular cross section to a rectangular one, 4 inches wide and 8 inches high.

In order to give uniform inlet-airflow distribution, two screens, 16 and 64 mesh, were placed between the transition and test section, 7 inches upstream from the first tube row. Another transition section changed the flow passage cross section to that of the 4-inch-diameter exhaust pipe. A control valve in the exhaust line was used to adjust the pressure level of the air in the test section. The entire test section and the inlet transition section were encased in a pressure shell 2 feet by 2 feet by 4 feet.

Electrical power was supplied through a 60-cycle, 128 kva, 120-volt a-c transformer and an 89-volt d-c saturable core reactor. This provided a power source that was controllable from essentially zero to 100 kilowatts. The electrical resistance of each tube in the test section was approximately 10 ohms; an applied voltage of 100 volts resulted in 1 kilowatt of power dissipation per tube.

Test Section

The test section (see fig. 2) was constructed of four stainless-steel walls with machine finished inside surfaces. The interior of the test section was 4 inches wide, 8 inches high, and 21 inches long. Holes were drilled through the sides on 0.842-inch transverse and longitudinal staggered centers for the 3/8-inch-diameter heater tubes. Blank "half tubes" were placed at alternate ends of the tube rows to reduce wall effects of discontinuity. There were 81 heated tubes, consisting of nine banks of nine tubes per bank.

Figure 3 is a schematic view of the test section. Temperature and total-pressure probes were placed before and after the test core as shown in figure 3. Four peripheral wall static-pressure taps were positioned in the same plane as the tips of the probes across the duct both at the inlet and outlet ends. Seven readings each of temperature, and total pressure, and four of the static pressure were available at the inlet to the test core; at the outlet there were 12 temperature and 12 total-pressure probes, and four static-pressure taps.

The insert of figure 3 illustrates the manner in which the heater tubes were passed through the wall. Ceramic spacers were used to secure the tubes in the horizontal direction. A certain amount of air leakage resulted from the clearance necessary for tube assembly through the wall. The escaping air, which pressurized the space between the test section and outer shell up to the operating pressure, minimized this leakage.

Tube Fabrication

The heater elements were fabricated from 3/8-inch-outside-diameter, 0.030-inch wall, stainless-steel tubing. Approximately 100 turns of 24 Nichrome V wire were made around a 5/16-inch mandril and placed inside the tube, which was then packed with alumina powder. The resistance of individual heaters differed from the average resistance by not more than ±5 percent. The powder served both to hold the heating coil in place and to provide electrical insulation between tube and wire. Studs (no. 10) were affixed to the ends of the heating wire to permit electrical connections. The tubes were swaged to compress the alumina powder. The insert of figure 3 illustrates the heater-tube construction. The tubes were $5\frac{1}{2}$ inches long; the nichrome heater coil was 4 inches long and was centered in the tube.

After data were obtained from the unfinned tubes, they were removed from the test section and finned. The 0.78-inch-diameter fins were fabricated from 0.020-inch stainless-steel sheet. The fins were attached to the tubes by furnace nicrobrazing; with 8 fins per inch, there were 31 in a 4-inch heated-tube length. Thermocouple lead tubes were fixed in place prior to the brazing operation. The brazing operation served to bond the fins to the tube, bond the thermocouple tube to the heater tube, and give a good tube-wall thermocouple junction.

Instrumentation

Figures 4 and 5 show the thermocouple instrumentation pattern and tube thermocouple instrumentation, respectively, of the unfinned and finned tubes.

Unfinned tubes. - Figure 4(a) shows the locations of the 65 Chromel-Alumel thermocouples used to determine tube-wall temperatures. All thermocouples, with the obvious exception of those on tube 10, were placed at the forward stagnation point.

The surface temperature of the unfinned tubes was measured by thermocouples placed on the tube surface. The thermocouple junction was spot welded to the tube surface as shown in figure 5(a). From this junction the 30-mil lead wires were extended 1/2 inch along the tube surface. The insulated lead wires were anchored by a wire bracket to the tube surface

and then removed by passing them vertically through the airstream to the wall of the test section.

An experimental test was conducted on a single tube to determine the magnitude of thermocouple error incurred through conduction losses along the lead wires. Heat-transfer data were obtained by using a tube thermocoupled in the previous manner. The thermocouple was then removed and replaced by a second one. Figure 5(a) illustrates the two thermocoupling techniques. The 3-mil lead wires of the second thermocouple were buried for a distance of 1 inch in insulated grooves in the tube wall. The junction of this couple was spotwelded in the same position as the first. Both couples were at the forward stagnation point for the tests. The heat-transfer measurements were repeated. The effect on Nusselt number was less than 8 percent. The same temperature and pressure instrumentation was used for both the finned- and unfinned-tube test cores.

As shown in figure 2 tube-surface thermocouple lead wires were extended vertically to the nearest half tube. A possibility existed that these wires, though extremely small compared with the tube diameter, would induce a static-pressure loss in addition to that caused by the tube bank. In order to determine the extent of this interference, isothermal pressure-drop measurements were made on the tube bank prior to tube-wall thermocouple installation. These tests were repeated after tube instrumentation. Within the data scatter, there was no significant increase in the friction coefficient due to the presence of the tube-wall thermocouple lead wires in the airstream. On the basis of these tests it was assumed that there was no measurable contribution to the heat-transfer coefficient.

Finned tubes. - Figure 4(b) shows the locations of 15 tube-wall thermocouples used in the finned-tube core. (No attempt was made to measure fin temperatures.)

The thermocouple lead wires were encased by 2-hole ceramic tubing that was inside a 0.020-inch-outside-diameter stainless-steel tube. This assembly was placed in a 0.020-inch-diameter semicircular groove that extended from the thermocouple junction to the nearest end of the tube being tested. The lead wires running from the end of the ceramic tube to the junction were insulated from the tube wall. The fins were notched to permit installation over the thermocouple-lead assembly. All thermocouple junctions were at the forward stagnation point. Figure 5(b) shows a thermocoupled finned tube.

DATA REDUCTION

Heat-Transfer Data of Unfinned Tubes

The heat-transfer film coefficient for air flowing normal to unfinned-tube banks was obtained from the following defining relation:

The heat gain of the air was calculated from the measured airflow rate, and the inlet and outlet temperatures[1]:

$$Q = wc_{p,b}(T_2 - T_1) \tag{2}$$

The mean surface-to-air temperature difference of equation (1) was determined from

$$\Delta T_m = (T_s - T_b) \tag{3}$$

where T_b was evaluated as the arithmetic average of T_1 and T_2.

An average tube surface temperature T_s was obtained from the 65 thermocouple readings by two methods. Successive application of graphical integration techniques yields: (1) an average surface temperature for each thermocoupled tube, (2) an average tube-bank surface temperature, and finally (3) an average core surface temperature. Average surface temperatures were also evaluated as the arithmetic average of all thermocouple readings. These two methods were compared for runs 105 and 108, and gave T_s values that differed by less than 3 percent. Local surface temperatures exhibited a random pattern throughout the test core due to variations in pitch, eccentricity of heater coils, and thermocouple accuracy. It was believed that a satisfactory treatment of these random variations was an arithmetic average of all thermocouple readings; these are given in table II.

The heat-transfer data for the comparison test of the thermocouple techniques illustrated in figure 5(a) are shown in figure 6. These single-tube data were obtained for the same range of air weight-flow rates per tube as the unfinned-tube heat-transfer data. The tests were run for surface temperatures of 760°, 960°, and 1160° R.

These data indicate that the use of exposed thermocouple leads results in an error of less than 8 percent in the heat-transfer parameter. Of greater importance than the amount of error, however, is the fact that this deviation is essentially independent of Reynolds number and surface temperature. Thus, although the correlated data to be presented are subject to error, the effect of physical-property variation indicated by the unfinned-tube heat-transfer data is unaffected by the surface-temperature deviation, and the use of film density places the data on a single line. Note that these results are for a single tube, and it is assumed that this thermocouple is representative of those in the test section. An estimate of the boundary-layer thickness at the forward stagnation point indicates that it is one-fourth of the thermocouple-wire diameter. Thus, a variation of thermocouple error could not result from some wires being

[1]Electrical power measurements permitted a heat balance, which was within 10 percent.

thermocouple error could not result from some wires being enveloped by the boundary layer; they were all in the free stream. With this reservation the unfinned-tube heat-transfer data do properly indicate the effect of physical-property variation.

Pressure-Drop Data of Unfinned Tubes

The following expression for the friction factor was used:

$$f = \frac{\Delta p_f}{4\left(\frac{L}{d_H}\right)\left(\frac{\rho_b V^2}{2g_c}\right)} \tag{4}$$

Numerically the quantity $(\rho_b V^2)$ was evaluated as (G^2/ρ_{av}), and as given in reference 3 (p.162), the ratio (L/d_H) was evaluated as the number of tube banks (9).

The friction pressure drop was calculated by subtracting the pressure drop associated with momentum change from the measured static-pressure drop according to the relation

$$\Delta p_f = \Delta p_{1-2} - \frac{G^2}{g_c}\left(\frac{1}{\rho_2} - \frac{1}{\rho_1}\right) \tag{5}$$

Heat-Transfer Data of Finned Tubes

The heat-transfer film coefficient for air flowing normal to finned-tube banks was obtained from

$$h \equiv \frac{Q}{\eta_o S \Delta T_m} \tag{6}$$

The heat gain Q and surface-to-air temperature difference are given by equations (2) and (3), respectively. The primary surface temperature was obtained by arithmetically averaging the 15 thermocouple readings.

The over-all surface efficiency η_o is related to the fin efficiency by (ref. 4, p. 9):

$$\eta_o = 1 - \frac{S_f}{S}(1 - \eta_f) \tag{7}$$

The fin efficiency η_f is defined in reference 7 as

$$\eta_f = \frac{\int_o^{S_f} (T_f - T_a)\,dS}{(T_s - T_a)S_f} \tag{8}$$

Reference 7 shows that the fin efficiency is a function of two parameters, the ratio (d_f/d_t) and (lm), where

$$m = \sqrt{\frac{2h}{k\,\delta}} \tag{9}$$

Figure 7 gives the fin-efficiency curve used herein. For the case investigated, $d_f/d_t = 2.08$. For ease of calculation, the exact equation of this curve was represented by an equation of the form

$$\eta_f = \frac{\tanh\,(lm)}{lm} - \varphi(lm) \tag{10}$$

For the range of interest, $\varphi(lm)$ was evaluated to be 0.09. Equation (10) gives η_f values that differ by less than 3 percent from the curve for

$$1.0 < lm < 2.2$$

The calculation of the film coefficient h requires an iteration procedure using equations (6), (7), and (10). An initial value of h was obtained from equation (6) by setting $\eta_o = 1$. This initial h was used to obtain η_f from equation (10). Equation (7) then gave an adjusted value of η_o, which was used to determine a second film coefficient. This procedure was repeated until two successive values of the film coefficient differed by less than 0.05 percent.

For this iteration procedure fin thermal conductivity was evaluated at the primary surface temperature T_s. The fin efficiency from the final iteration step was used to obtain an average fin temperature defined as:

$$T_{f,av} = T_b + \eta_f \Delta T \tag{11}$$

The fin thermal conductivity was then reevaluated at $T_{f,av}$ and the iteration procedure repeated to obtain a new film coefficient.

The fin efficiency curve shown in figure 7 is of theoretical derivation (ref. 7), and certain assumptions are involved. Among these are the following: a constant thermal conductivity throughout the fin, and a constant heat-transfer coefficient over the entire fin surface. The correlations presented herein are based on this curve, and are valid if these assumptions realistically represent the heat-transfer mechanism.

Pressure-Drop Data of Finned Tubes

The same basic equations were used for the finned-tube-core pressure-drop data as for the unfinned tubes. In equation (4), the term $4(L/d_H)$ was evaluated by a relation defined in reference 4 (p. 3)

$$4\left(\frac{L}{d_H}\right) = \left(\frac{S}{A}\right) \tag{12}$$

The core length L was evaluated as the distance from the fin leading edge of the first tube bank to the fin trailing edge of the last tube bank. The numerical values of all physical parameters for both cores are listed in table I.

Physical Properties

Physical properties of air used herein were taken from reference 8. Figure 8(a) shows two thermal conductivity curves. One is from reference 8; the other is arbitrarily (see ref. 1) prescribed to vary as the square root of the absolute temperature, and to have the same reference temperature (530° R) value as that of reference 8. Figure 8(b) shows a Prandtl number curve corresponding to both thermal conductivities. For the conditions of these tests (Mach numbers less than 0.2), static and total temperatures were essentially equal, and all properties, including density, were evaluated using temperatures indicated by the airstream probes.

The thermal conductivity of type 347 stainless steel used for fin efficiency evaluation was taken from reference 9. The thermal conductivity - temperature relation for the temperature range 600° to 1400° R is

$$k = 6.03 + 0.00486T$$

RESULTS AND DISCUSSION

Heat-Transfer Data of Unfinned Tubes

The unfinned-tube heat-transfer data were initially plotted using bulk density. Figure 9(a) shows a plot of Nusselt number Nu divided by Prandtl number Pr to the 0.4 power against Reynolds number. Specific heat, viscosity, and the thermal conductivity of reference 8 are evaluated at the film temperature. Figure 9(a) shows that this type of correlation is not satisfactory. The data indicate a trend with respect to surface temperature.

In order to remove this effect of physical-property variation and to obtain a correlation independent of surface temperature, the density was also evaluated at the film temperature midway between the air bulk temperature and T_s. This film Reynolds number is defined as

$$Re_f = \left(\frac{d_t V \rho_f}{\mu_f}\right) \tag{13}$$

Figure 9(b) shows a replot of the data using this correlation. The data fall on a single line. The recommended curve of reference 3 (p. 273, $X_L = X_T = 2.24$)) is included for comparison. These data, all for an air inlet temperature of approximately 530° R, cover a range of surface-to-bulk temperature ratios from 1.64 to 2.36. Figure 9(b) indicates that the heat-transfer correlation procedure used in reference 1 for flow through tubes is also valid for flow across the unfinned-tube banks.

Pressure-Drop Data of Unfinned Tubes

Figure 9(a) shows a plot of the friction coefficient f, calculated from equation (4), against the bulk density Reynolds number. An apparent separation of data corresponding to various surface temperatures exists, but because of scatter it is less clearly defined than the separation for the heat-transfer data. Figure 9(a) indicates that in addition to the flow parameter ($d_t V \rho_b / \mu_f$), the friction coefficient is a function of the surface-to-bulk temperature ratio (T_s/T_b). The friction coefficients for flow across unfinned-tube banks increase with increasing surface-to-bulk temperature ratio. This is in direct contrast to results for flow through tubes, where the friction coefficients decreased with increasing surface-to-bulk temperature ratio.

Figure 9(b) shows the results of evaluating density in Reynolds number at the film temperature (eq. (13)). The friction coefficient f is again calculated from equation (4). The recommended curve of reference 3 (p. 163) is also shown. As is shown in figure 9(b), the use of a film density Reynolds number removes the effect of physical-property variation. In order to effect a satisfactory correlation of friction data for flow through tubes (ref. 1), it was necessary to use film density in the definition of the friction coefficient as well as in Reynolds number.

Heat-Transfer Data of Finned Tubes

Figure 10(a) shows the heat-transfer data with density evaluated at the bulk air temperature T_b. As in the case of unfinned tubes, this type of correlation is inadequate. The data show a definite separation according to surface temperature. These data, at an air inlet temperature of approximately 530° F, cover a range of surface-to-bulk temperature ratios from 1.07 to 1.6. The surface temperatures listed in table II are arithmetic averages of all the thermocouple-tube readings, and are primary surface temperatures.

The same procedure successful for the unfinned-tube data was employed to remove the temperature-level effect. Figure 10(b) shows the heat-transfer data with all properties, including density, evaluated at the film temperature. This film correlation is not sufficient; the substantial spread remaining in the data shows an ordered relation with T_s.

By using a correlation procedure suggested in reference 1, the data were evaluated using the arbitrary thermal conductivity (fig. 8(a)) and corresponding Prandtl number (fig. 8(b)). The results are shown in figure 10(c). The variation with surface temperature is reduced but still apparent.

With this same thermal conductivity k^*, the data were recalculated by evaluating all properties at the primary surface temperature T_s. The results are shown in figure 10(d). Although a slight trend still exists, the data are acceptably represented by a single line.

The data were also evaluated at an average over-all surface temperature defined by the relation

$$T_{s,av} = T_b + \eta_o \Delta T_m \tag{14}$$

Using this temperature, an average over-all film temperature was evaluated as

$$T_{f,av} = \frac{1}{2}(T_{s,av} + T_b) \tag{15}$$

Both of these temperatures were used, but the correlations were not satisfactory.

Although the evaluation of properties at the primary surface temperature rather than some over-all surface average temperature is difficult to justify, this procedure yields the best correlation of the test data. Heat-transfer data from other finned-tube cores, covering a different range of fin efficiencies, for example, would permit a more conclusive over-all correlation.

Pressure-Drop Data of Finned Tubes

Figure 10(a) shows the friction coefficient f as defined by equation (4) plotted against bulk density Reynolds number. No significant trend with respect to surface temperature level is apparent. Figure 10(b) shows a replot of the same f (eq. (4)) against a film density Reynolds number. This corresponds to figure 9(b) which gave an improved correlation for the unfinned tubes. Figure 10(b), however, shows that the evaluation of the density in the Reynolds number a film temperature results in an increased deviation from a single-line correlation. The data for flow across finned tubes are satisfactorily correlated by the use of a bulk density in the friction coefficient and Reynolds number.

Since the effect of the temperature at which the viscosity is evaluated is slight, the inherent scatter of the data prevents any conclusion as to whether a bulk or film temperature is more satisfactory. It should be noted that for the fin efficiencies encountered (approx. 50 percent), the ratio $(T_{f,av}/T_b)$ does not exceed 1.17. Any modification of the friction coefficient and/or Reynolds number on this basis would result in a

correlation essentially the same as shown in figure 10(a). It is possible, that for a configuration yielding appreciably higher fin efficiencies, a correlation on the basis of $T_{f,av}$ would be necessary.

SUMMARY OF RESULTS

Measurements were made of average heat-transfer and friction coefficients for heat addition to air flowing normal to staggered banks of electrically heated finned and unfinned tubes for variable property conditions. A Reynolds number range from 2000 to 35,000 was investigated for an inlet air temperature of 530° R, and surface temperatures from 660° to 1400° R. Isothermal friction coefficients are also reported. Heat-transfer and friction correlations are shown for physical properties evaluated at bulk, film, and surface temperatures. The following results are indicated for finned and unfinned tubes.

1. A single-line correlation of the unfinned-tube heat-transfer data is obtained by evaluating all physical properties, including density, at the film temperature.

2. The unfinned-tube pressure-drop data are correlated by the use of film density and film viscosity in Reynolds number, and bulk density in the friction coefficient.

3. A single-line correlation of the finned-tube heat-transfer data is effected by evaluating all properties, including density, at the primary surface temperature, and utilizing an arbitrary thermal conductivity for air given by $k^* = 0.015\sqrt{T/530}$, where T is absolute temperature.

4. Little or no physical-property variation is apparent in the finned-tube pressure-drop data, and a correlation is obtained by using a bulk density in both the Reynolds number and friction coefficient.

CONCLUSIONS

The data presented herein are for an individual finned-core configuration and are not intended as general correlations. Additional data are necessary for other core configurations. This is particularly true for finned tubes, because the effects of physical-property variation may well be a function of core geometry.

Lewis Research Center
National Aeronautics and Space Administration
Cleveland, Ohio, August 27, 1958

REFERENCES

1. Humble, Leroy V., Lowdermilk, Warren H., and Desmon, Leland G.: Measurements of Average Heat-Transfer and Friction Coefficients for Subsonic Flow of Air in Smooth Tubes at High Surface and Fluid Temperatures. NACA Rep. 1020, 1951. (Supersedes NACA RM's E7L31, E8L03, E50E23, and E50H23.)

2. Deissler, R. G., and Eian, C. S.: Analytical and Experimental Investigation of Fully Developed Turbulent Flow of Air in a Smooth Tube with Heat Transfer with Variable Fluid Properties. NACA TN 2629, 1952.

3. McAdams, William H.: Heat Transmission. Third ed., McGraw-Hill Book Co., Inc., 1954.

4. Kays, W. M., and London, A. L.: Compact Heat Exchangers. The National Press, Palo Alto (Calif.), 1955.

5. Gunter, A. Y., and Shaw, W. A.: A General Correlation of Friction Factors for Various Types of Surfaces in Crossflow. Trans. ASME, vol. 67, no. 8, Nov. 1945, pp. 643-660.

6. Jameson, S. L.: Tube Spacing in Finned-Tube Banks. Trans. ASME, vol. 67, no. 8, Nov. 1945, pp. 633-642.

7. Gardner, Karl A.: Efficiency of Extended Surface. Trans. ASME, vol. 67, no. 8, Nov. 1945, pp. 621-631.

8. Hilsenrath, Joseph, et al.: Tables of Thermal Properties of Gases. Cir. 564, NBS, Nov. 1, 1955.

9. Perry, John H., ed.: Chemical Engineers' Handbook. Third ed., McGraw-Hill Book Co., Inc., 1950, p. 456.

TABLE I. - TEST-CORE PHYSICAL CONSTANTS

	Unfinned tube	Finned tube
Frontal area, sq ft	0.222	0.222
Minimum flow area, A, sq ft	.123	.107
Fin diameter, d_f, in.	-----	.78
Hydraulic diameter, d_H, in.	not used	.214
Tube diameter, d_t, in.	.375	.375
Fin height, l, in.	-----	.2025
Core length, L, in.	7.12	7.52
Number of banks	9	9
Fins per inch, $in.^{-1}$	-----	8
Heated tubes per bank	9	9
Fin surface area, S_f, sq ft	-----	12.9
Total surface area, S, sq ft	2.65	15.1
Longitudinal tube spacing, in.	.842	.842
Transverse tube spacing, in.	.842	.842
Fin thickness, δ, in.	-----	.020

TABLE II. - BASIC DATA

(a) Unfinned tube

Run	w, lb/sec	T_1, °F	T_2, °F	T_s, °F	p_1, $\frac{lb}{sq\ in.\ abs}$	Δp_{1-2}, $\frac{lb}{sq\ in.\ abs}$
Isothermal pressure-drop data						
96	0.35	75			14.71	0.0398
97	.49	75			15.22	.0688
98	.66	75			15.74	.116
99	.82	75			16.27	.181
100	1.08	75			17.29	.268
101	1.51	73			17.92	.507
102	2.06	73			20.17	.702
103	2.43	73			22.17	.843
Heat-transfer and pressure-drop data						
104	0.46	70	168	487	15.51	0.07964
105	.57	67.6	162.6	485	15.93	.1184
106	.83	68.7	155	490	17.14	.2136
107	1.19	69.6	146	486	19.80	.3819
108	1.83	70	146	520	25.22	.6426
109	.46	73.7	226.2	695	15.30	.0869
110	.76	73.9	204.8	703	15.95	.2172
111	1.05	72.6	195.2	705	17.32	.3892
112	1.62	66.3	176.7	708	20.44	.7095
113	.42	82.3	297	956	15.5	.0833
114	.70	71.7	254.5	944	16.7	.197
115	1.0	63.7	228.1	921	18.6	.340
116	2.12	67.9	134	491	21.7	1.008
117	2.74	62	131.1	496	24.9	1.275
118	2.62	73.7	164.3	704	24.35	1.347
119	2.17	74.1	173.7	719	22.18	1.13
120	1.49	78.3	228.7	982	18.9	.778
[a]121	1.94	79.0	199.4	944	21.1	1.01

[a]Eleven tubes burned out on final heat-transfer run, use total heat-transfer surface of 70 tubes.

TABLE II. - Continued. BASIC DATA

(b) Finned tube

Run	w, lb/sec	T_1, °F	T_2, °F	T_s, °F	p_1, lb/sq in. abs	Δp_{1-2}, lb/sq in. abs
Heat-transfer and pressure-drop data						
142	0.34	79	124.0	143.8	14.99	0.141
143	.49	79	117.8	142.0	15.27	.239
144	.25	80	132.6	146.0	14.96	.0616
145	2.39	84	102.4	140.3	24.23	2.84
146	2.14	84	103.3	139.3	23.13	2.52
147	1.89	85	104.6	139.2	21.36	2.11
148	1.66	85	105.7	137.4	20.06	1.73
149	1.40	85	108.7	140.1	18.70	1.38
150	1.10	86	111.7	142.0	17.10	.998
151	.96	86	114.1	143.4	17.00	.763
152	.84	86	113.0	139.5	16.50	.648
153	.72	86	115.1	141.4	16.17	.506
154	.64	86	116.7	141.1	15.84	.384
155	.59	86	117.2	140.9	15.82	.333
156	2.41	87.3	183.2	415.0	25.19	3.14
157	.49	88.3	295.6	434.8	15.57	.293
158	.68	88.3	265.7	428.7	16.12	.518
159	.25	82	365.0	451.0	14.96	.076
160	.34	81	313.0	431.0	14.99	.166
161	.59	81	277.0	432.0	15.56	.369
162	.76	81	257.0	427.0	16.19	.605
163	.86	83	249.0	436.0	16.54	.728
164	.96	84	241.0	434.0	17.02	.883
165	1.1	84	237.0	449.0	17.59	1.096
166	1.24	88	226.0	428.0	18.16	1.313
167	1.4	84	214.0	427.0	17.28	1.531
168	1.67	85	201.0	423.0	20.57	1.987
169	1.88	85	194.0	420.0	21.78	2.356
170	2.17	85	185.0.	412.0	23.62	2.77
171	1.11	85	303.0	548.0	17.83	1.151
172	.97	86	325.0	599.0	18.32	.956
173	.86	85	324.0	583.0	16.94	.771
174	.76	86	337.0	584.0	16.44	.777
175	.68	86	348.0	578.0	16.19	.561
176	.59	87	363.0	587.0	16.82	.427
177	.49	88	386.0	590.0	15.78	.326
178	.34	90	457.0	612.0	15.23	.159
179	.25	91	477.0	590.0	15.22	.0905

TABLE II. - Concluded. BASIC DATA

(b) Concluded. Finned tube

Run	w, lb/sec	T_1, °F	T_2, °F	T_s, °F	p_1, lb/sq in. abs	Δp_{1-2}, lb/sq in. abs
Isothermal pressure-drop data						
181	0.25	81			14.92	0.058
182	.34	81			14.98	.116
183	.43	81			15.16	.170
184	.49	81			15.26	.206
185	.54	81			15.40	.268
186	.58	81			15.46	.312
187	.68	81			15.70	.427
188	.76	81			15.96	.532
189	.84	81			16.25	.615
190	.96	81			16.60	.743
191	1.12	81			17.14	1.01
192	1.37	81			18.28	1.32
193	1.72	81			20.13	1.80
194	1.99	81			21.50	2.25
195	2.45	81			24.30	2.87
196	.110	76			14.70	.00724
197	.155	76			14.70	.0271
198	.187	83			14.71	.038
199	.215	76			14.71	.0545
200	.240	76			14.72	.0615
201	.262	76			14.72	.0778
202	.284	78			14.72	.0869
203	.303	78			14.72	.0977
204	.340	78			14.74	.1232
205	.370	79			14.95	.1412
206	.400	79			15.01	.159
207	.428	79			15.12	.181
208	.455	80			15.18	.203
209	.480	80			15.27	.225
210	.540	80			15.30	.268
211	.590	81			15.42	.311
212	.680	82			15.63	.409
213	.590	82			15.57	.311
214	.480	82			15.47	.221
215	.415	82			15.31	.174
216	.340	83			15.03	.116
217	.240	83			14.97	.0616
218	.187	83			14.69	.0399
219	.110	83			14.70	.01268

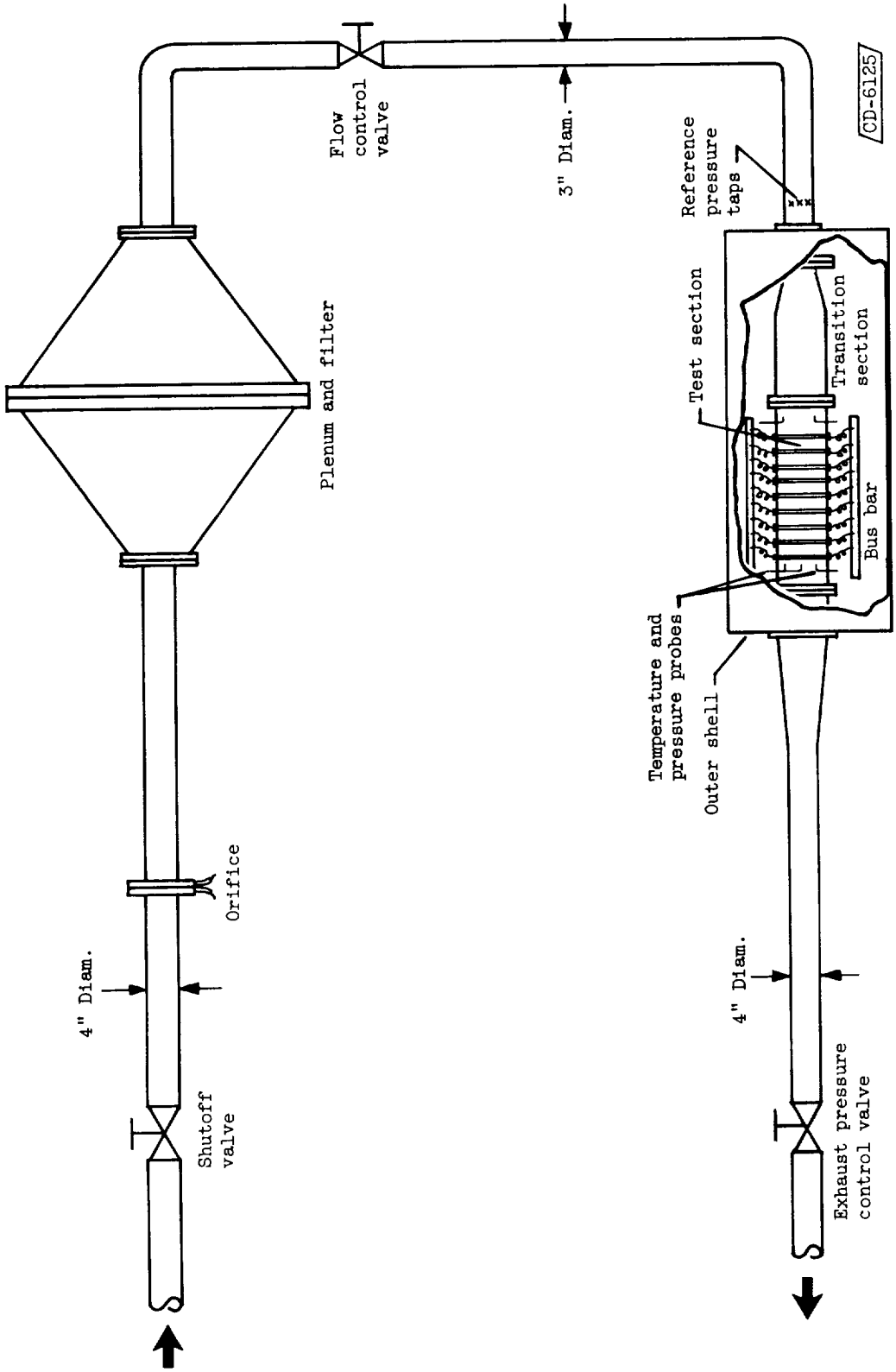

Figure 1. - Schematic drawing of test apparatus.

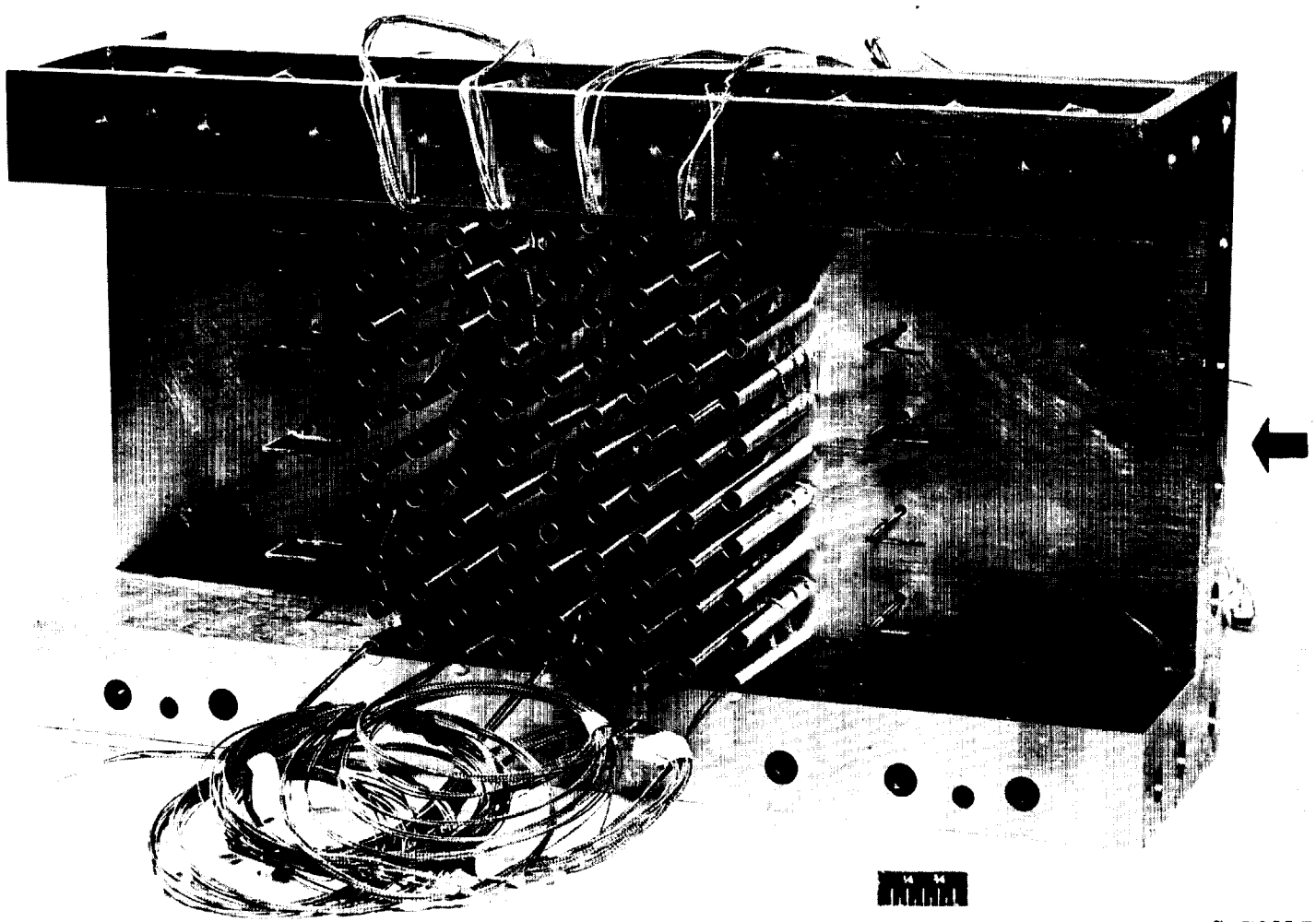

C-36815

Figure 2. - Test section showing instrumentation probes and thermocouple lead wires.

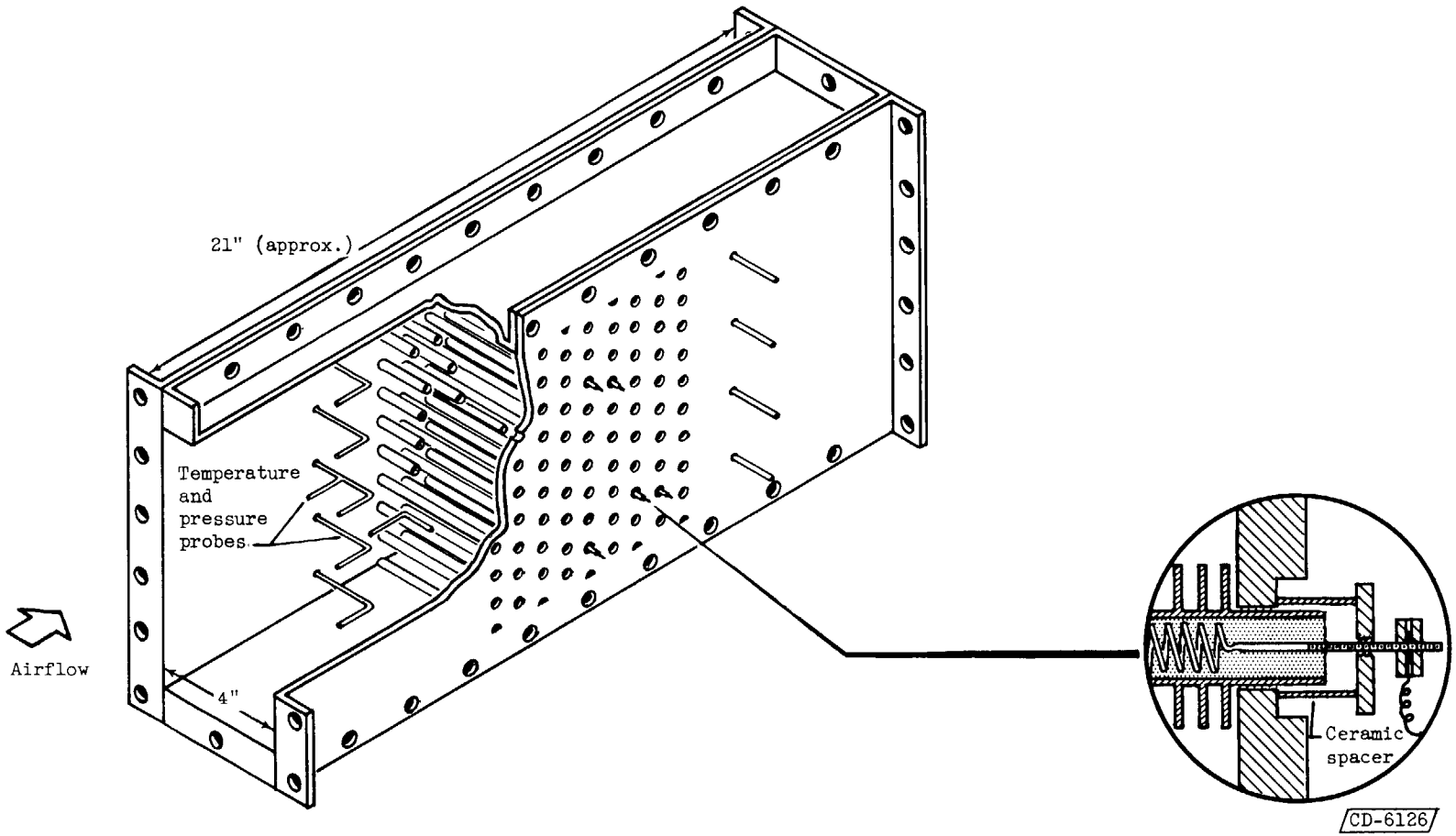

Figure 3. - Schematic picture of test section showing tube-through-wall connection.

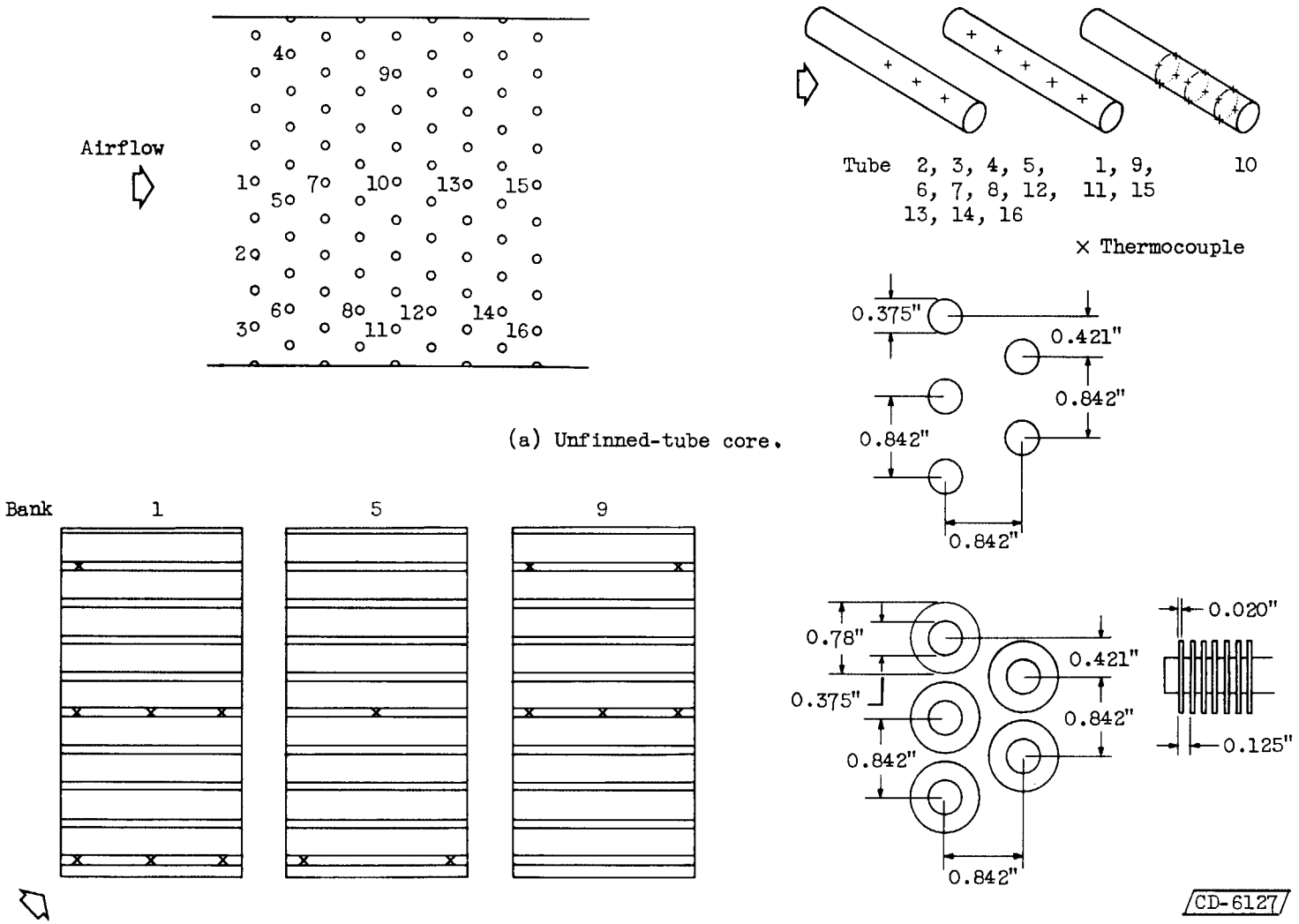

(a) Unfinned-tube core.

(b) Finned-tube core.

Figure 4. - Thermocouple instrumentation pattern.

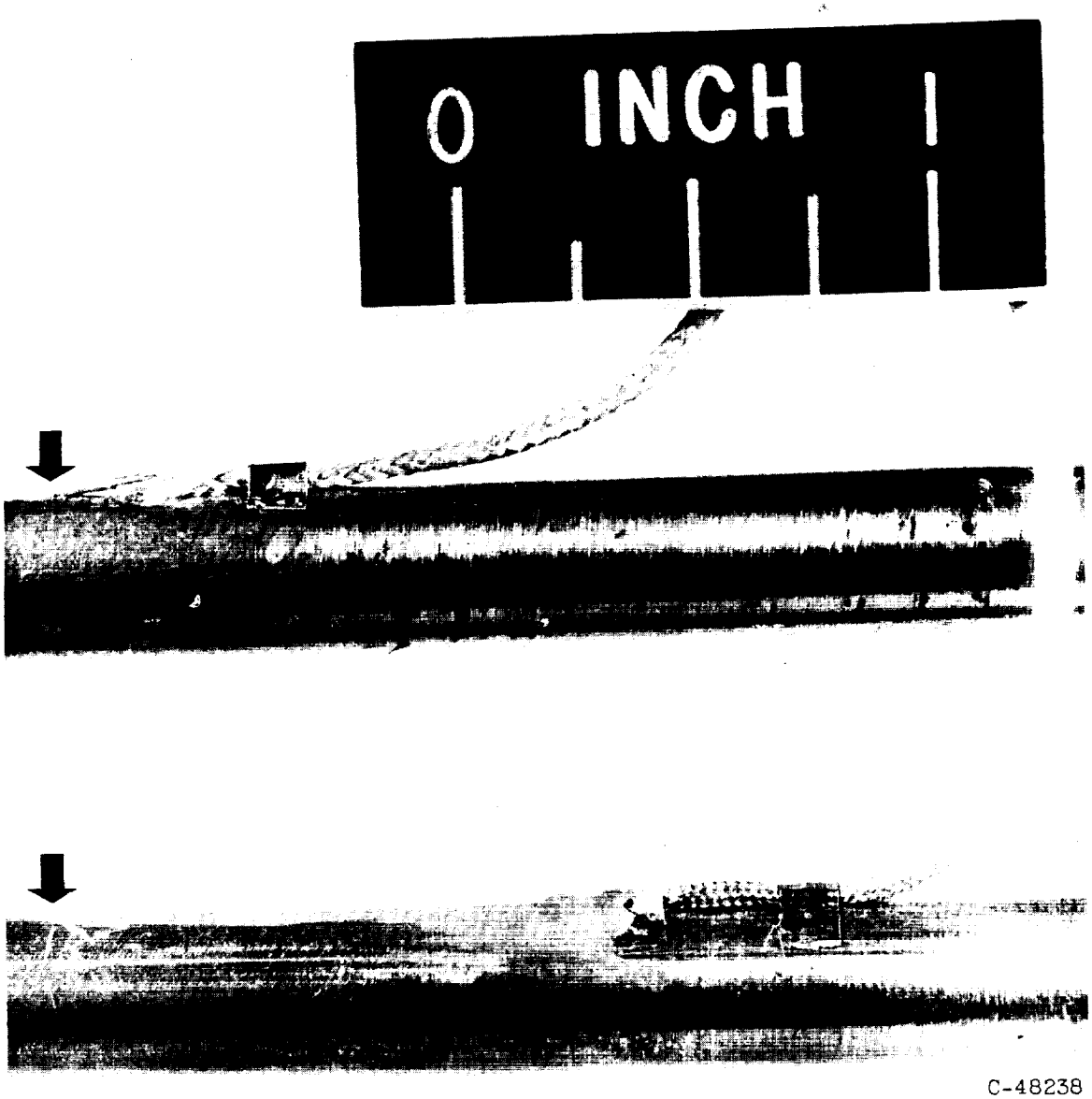

(a) Unfinned tube; exposed and buried leads.

Figure 5. - Tube thermocouple instrumentation.

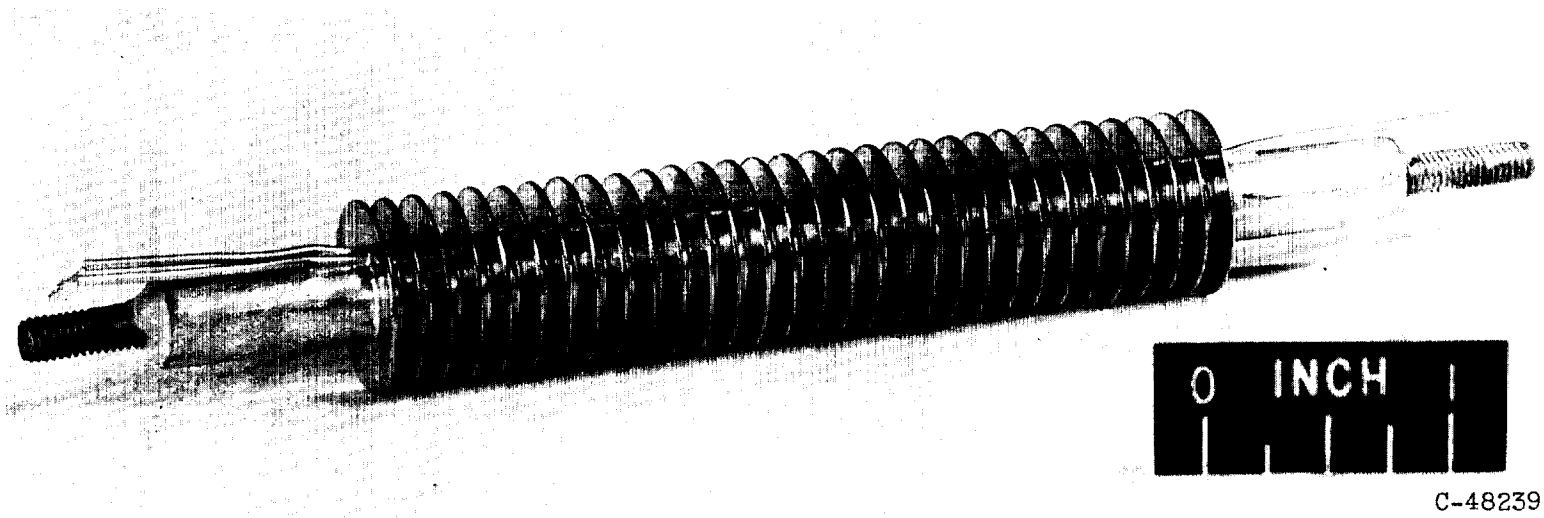

(b) Finned tube.

Figure 5. - Concluded. Tube thermocouple instrumentation.

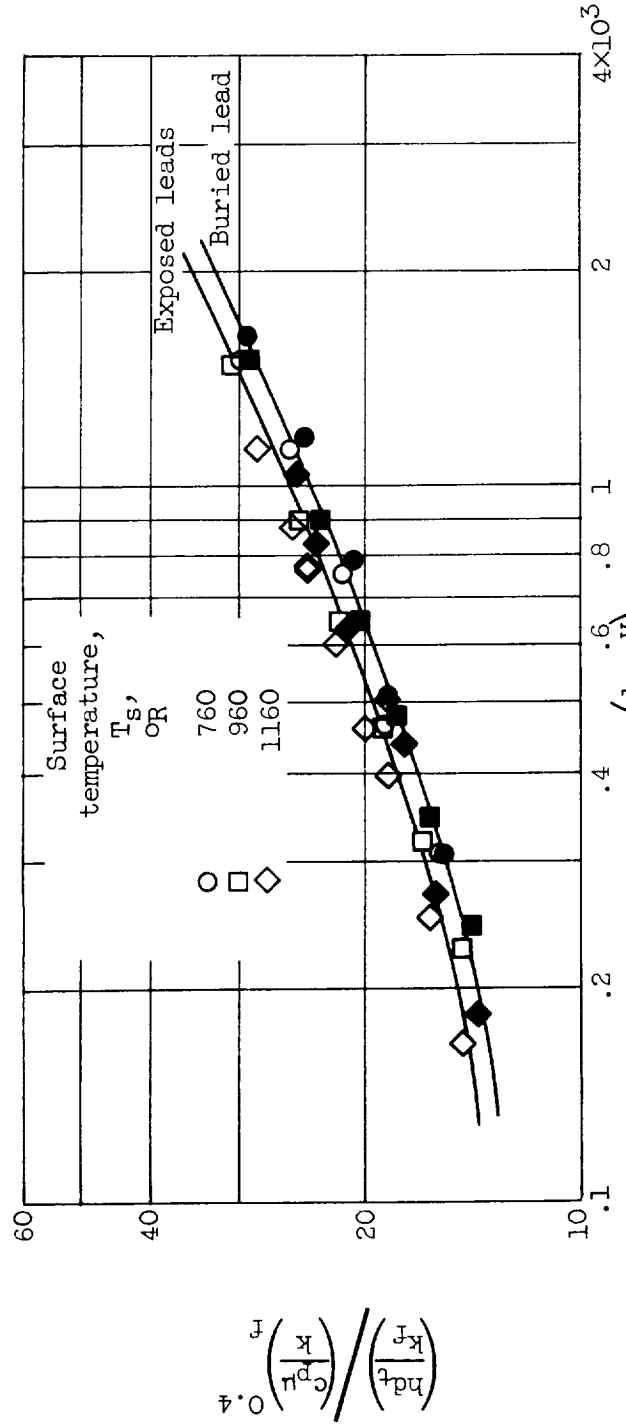

Figure 6. - Single-tube heat-transfer data for two surface-thermocouple techniques.

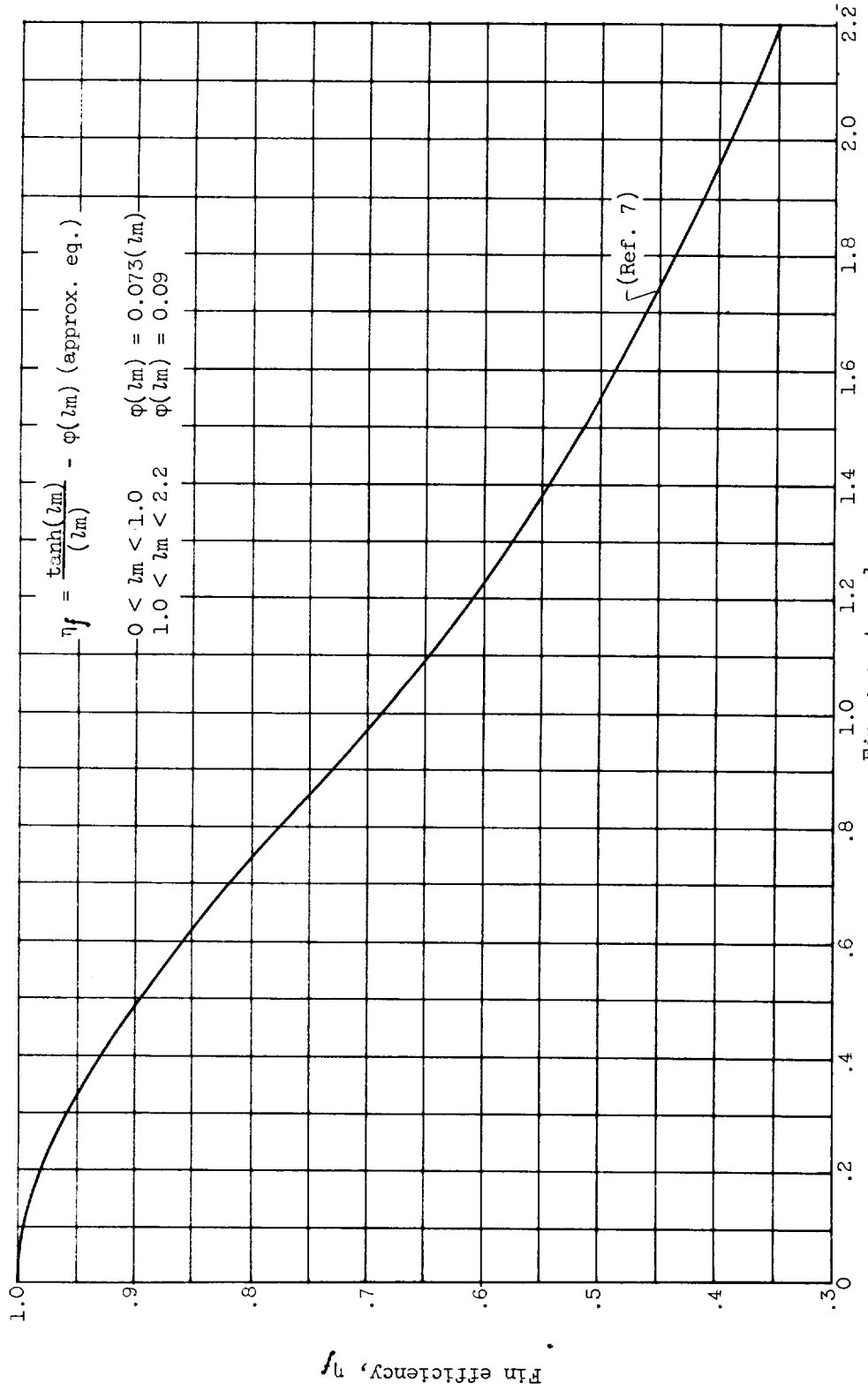

Figure 7. - Variation of fin efficiency with fin parameter for d_f/d_t of 2.08.

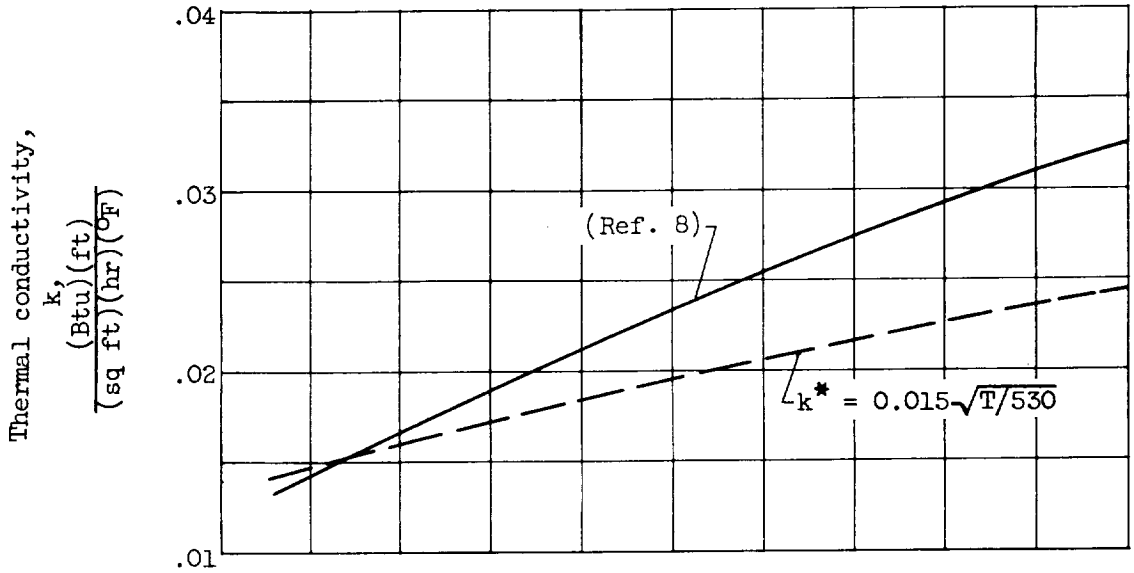

(a) Thermal conductivity.

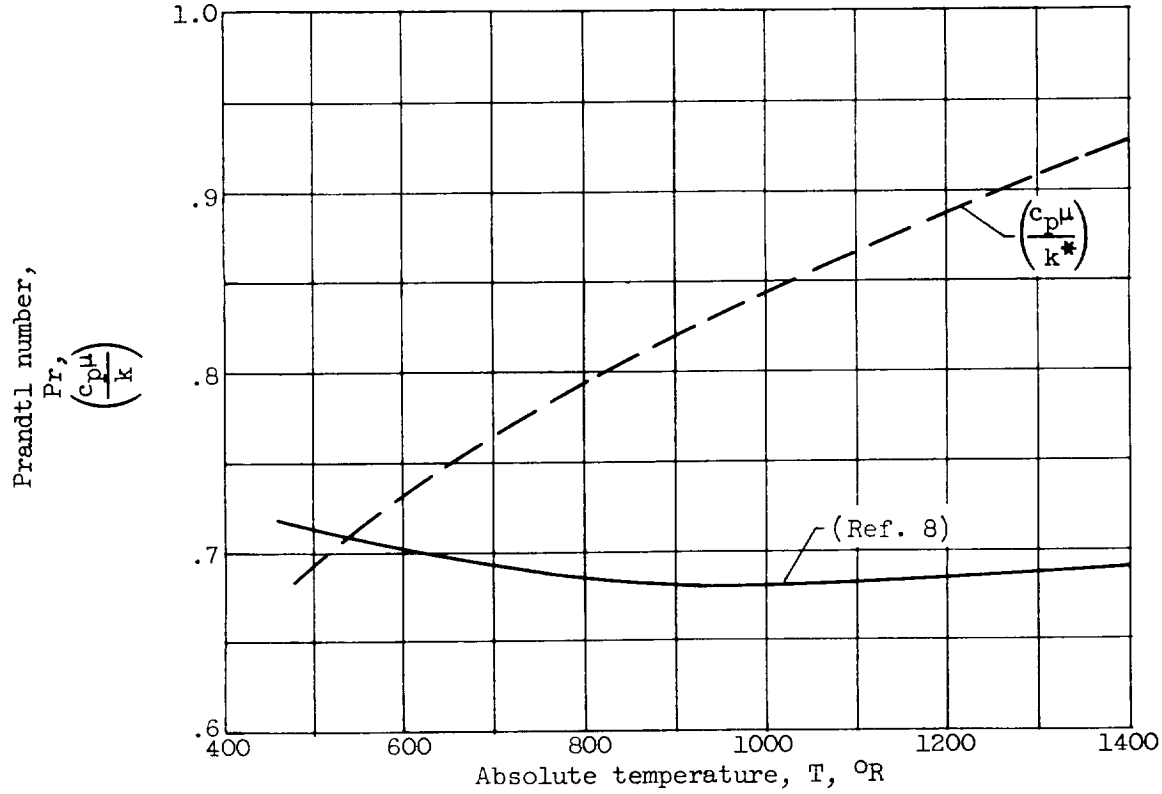

(b) Prandtl number.

Figure 8. - Physical properties of air.

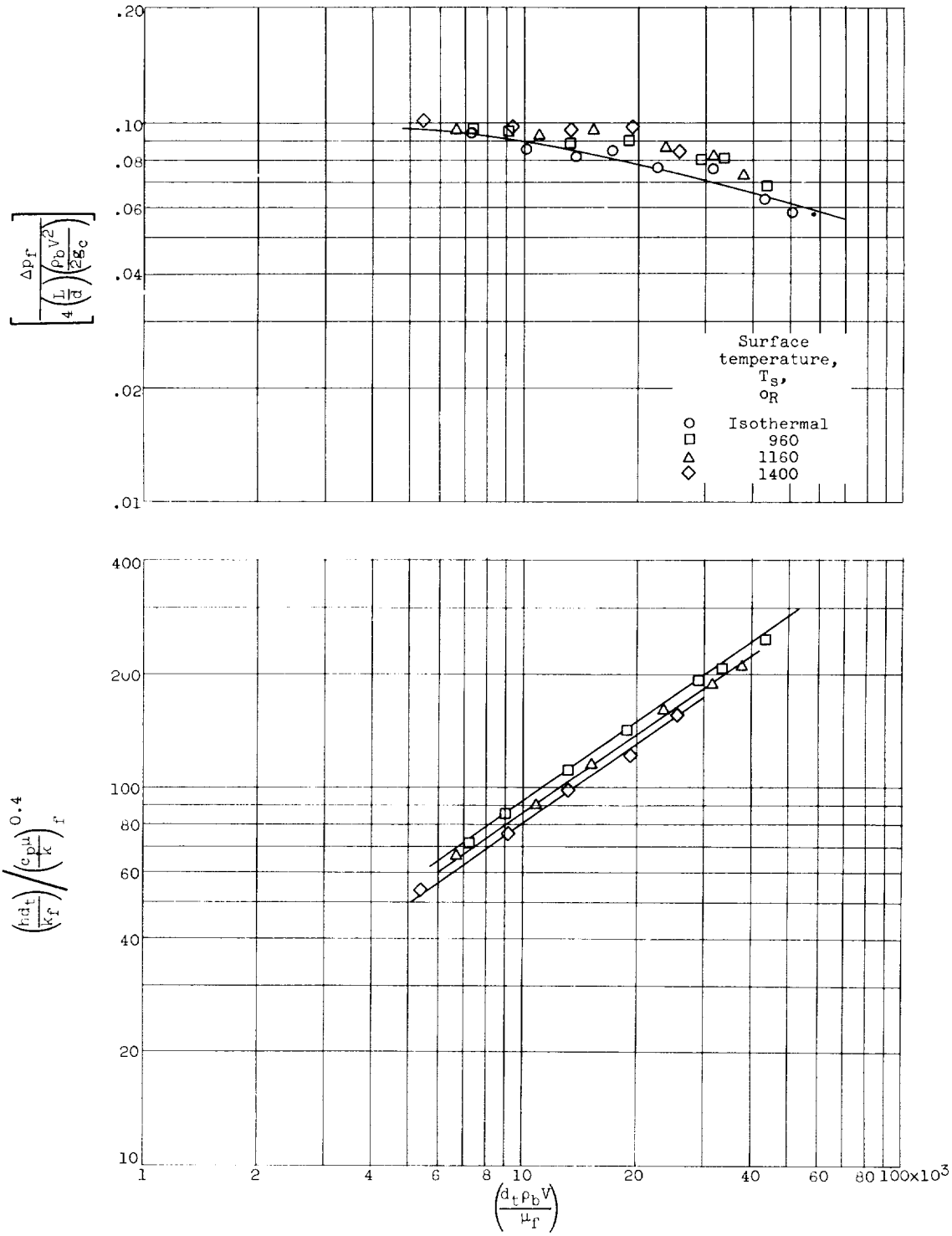

(a) Bulk-density correlation.

Figure 9. - Heat-transfer and friction data of unfinned tubes.

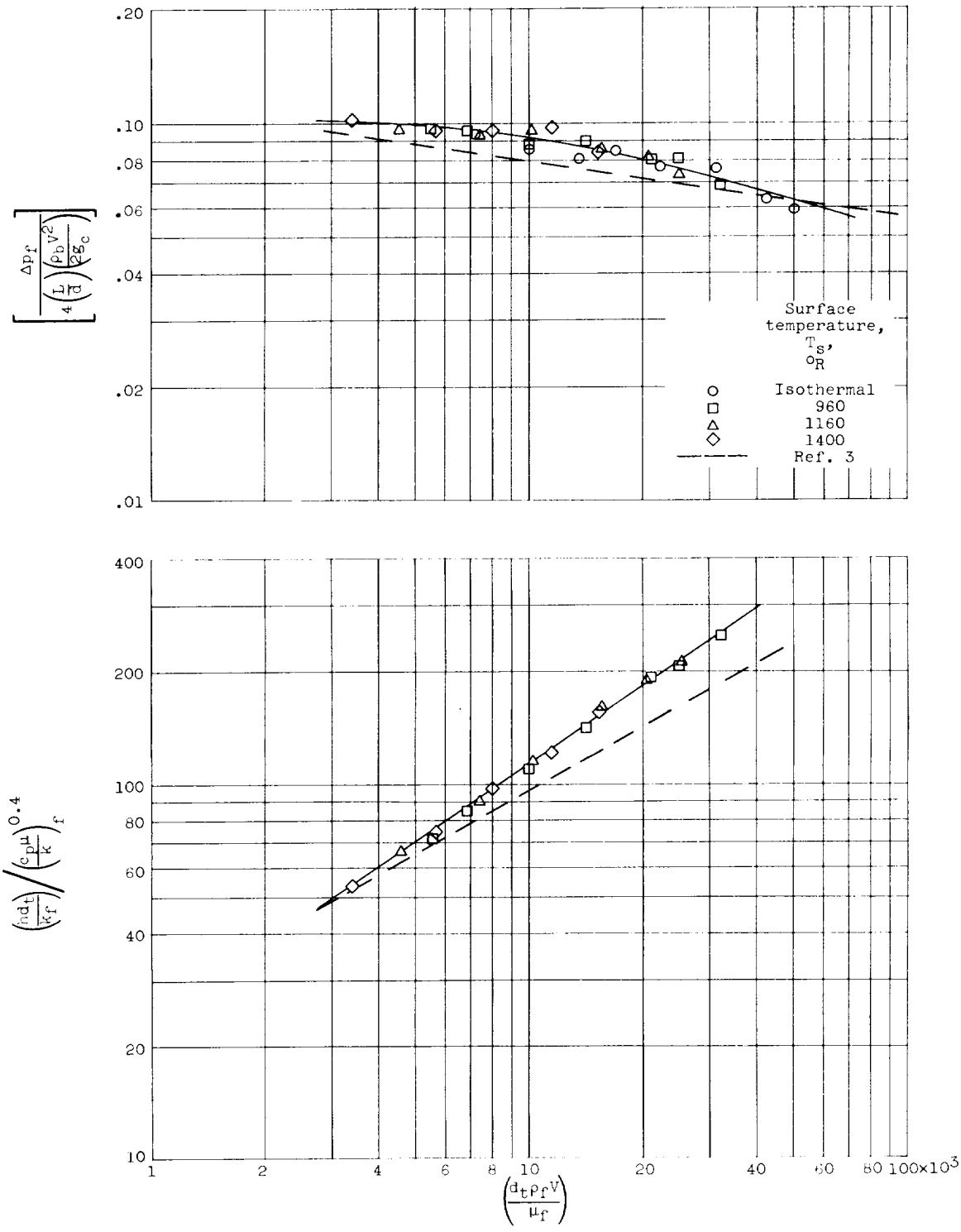

(b) Film-density correlation.

Figure 9. - Concluded. Heat-transfer and friction data of unfinned tubes.

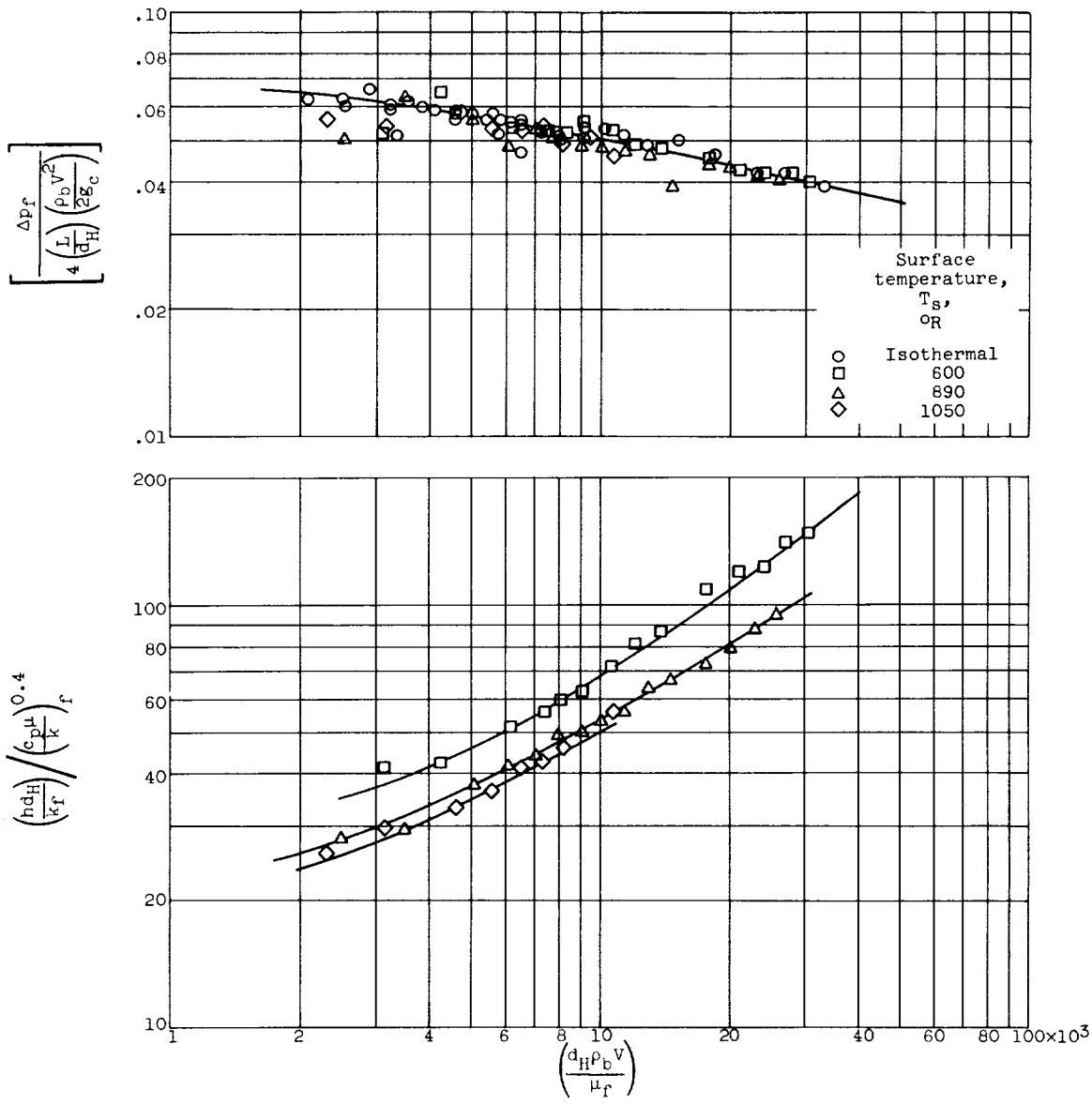

(a) Bulk-density correlation.

Figure 10. - Heat-transfer and friction data of finned tubes.

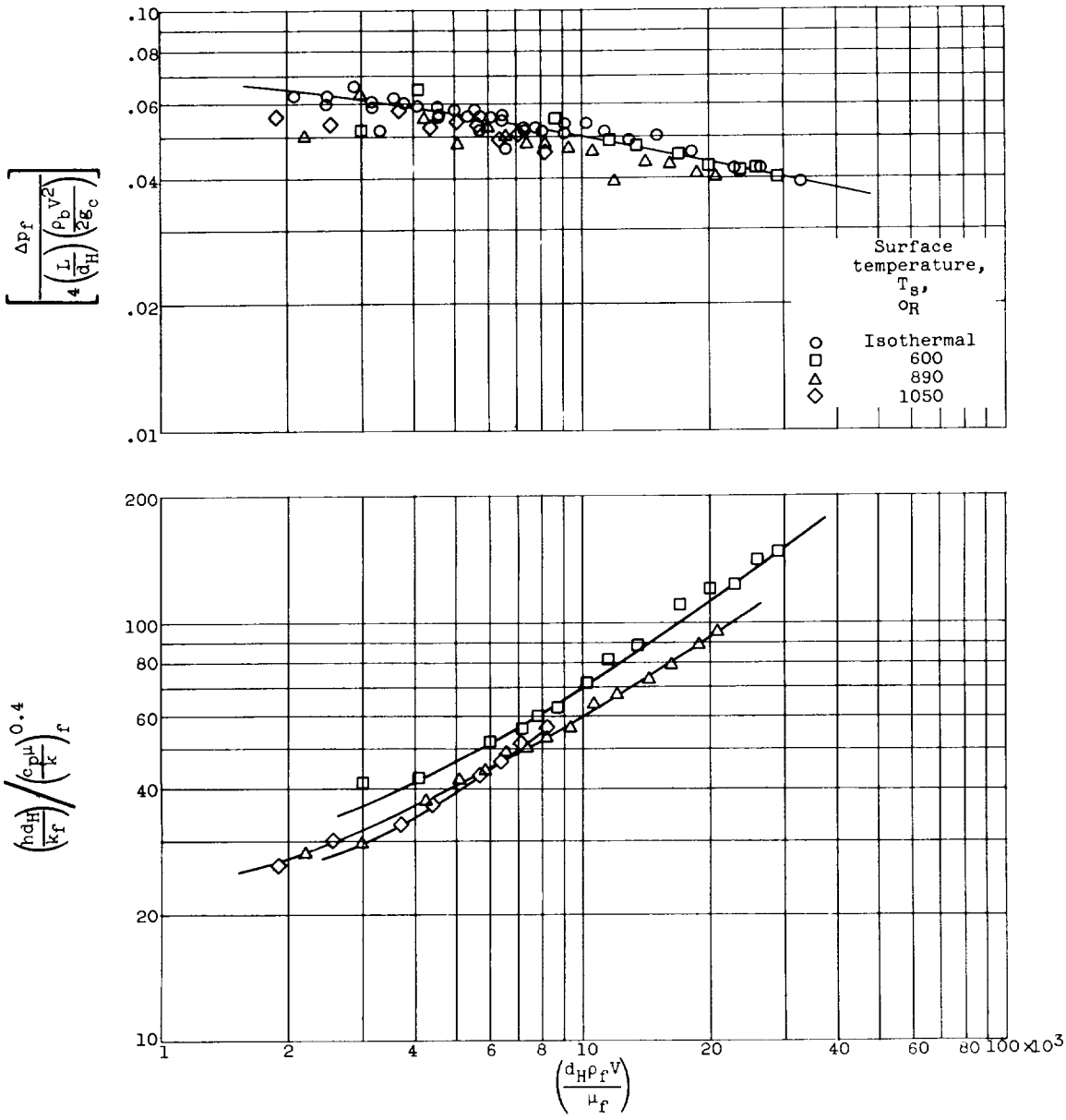

(b) Film-density correlation, thermal conductivity of reference 8.

Figure 10. - Continued. Heat-transfer and friction data for finned tubes.

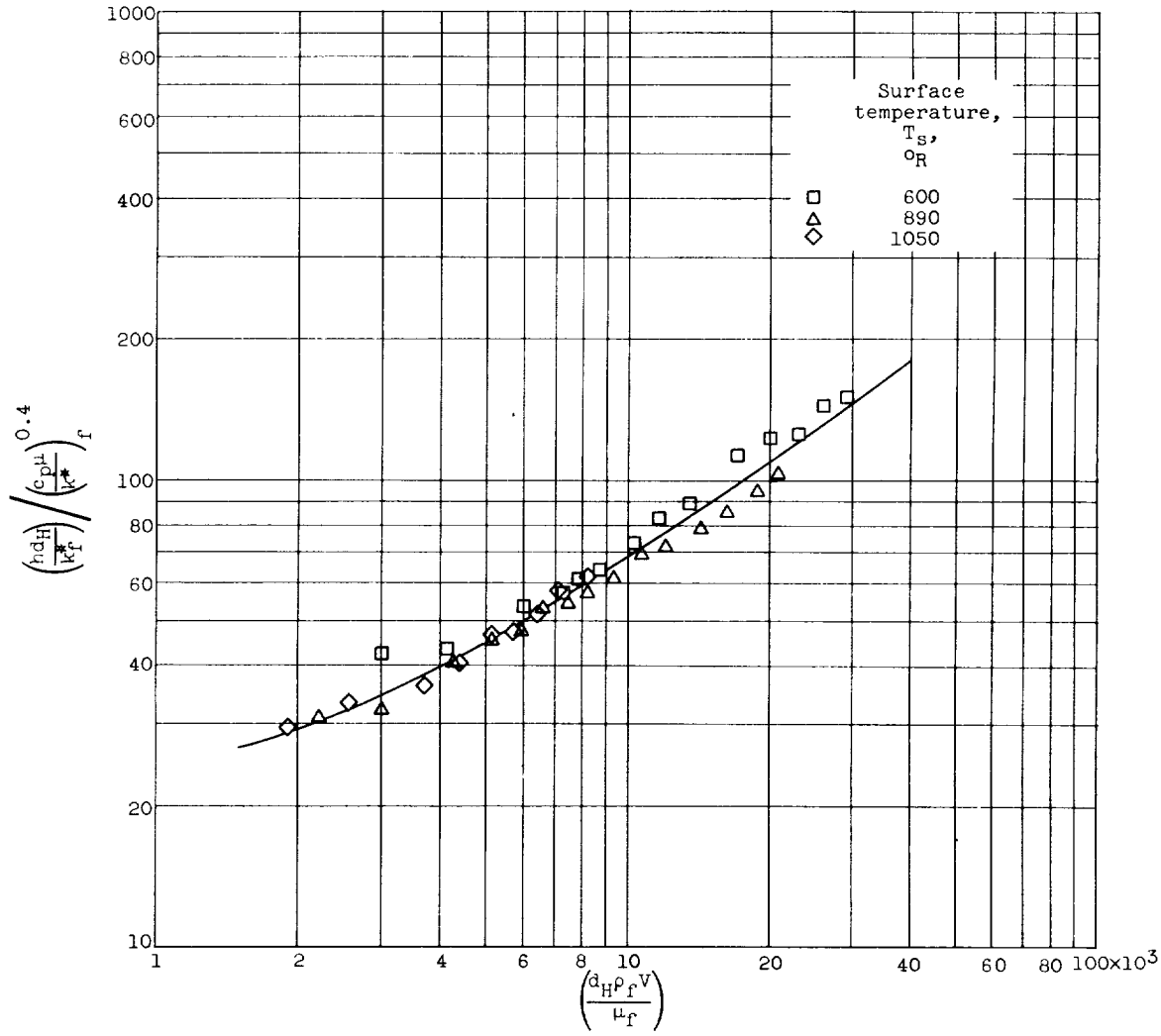

(c) Film-density correlation, $k^* = 0.015\sqrt{T/530}$.

Figure 10. - Continued. Heat-transfer and friction data for finned tubes.

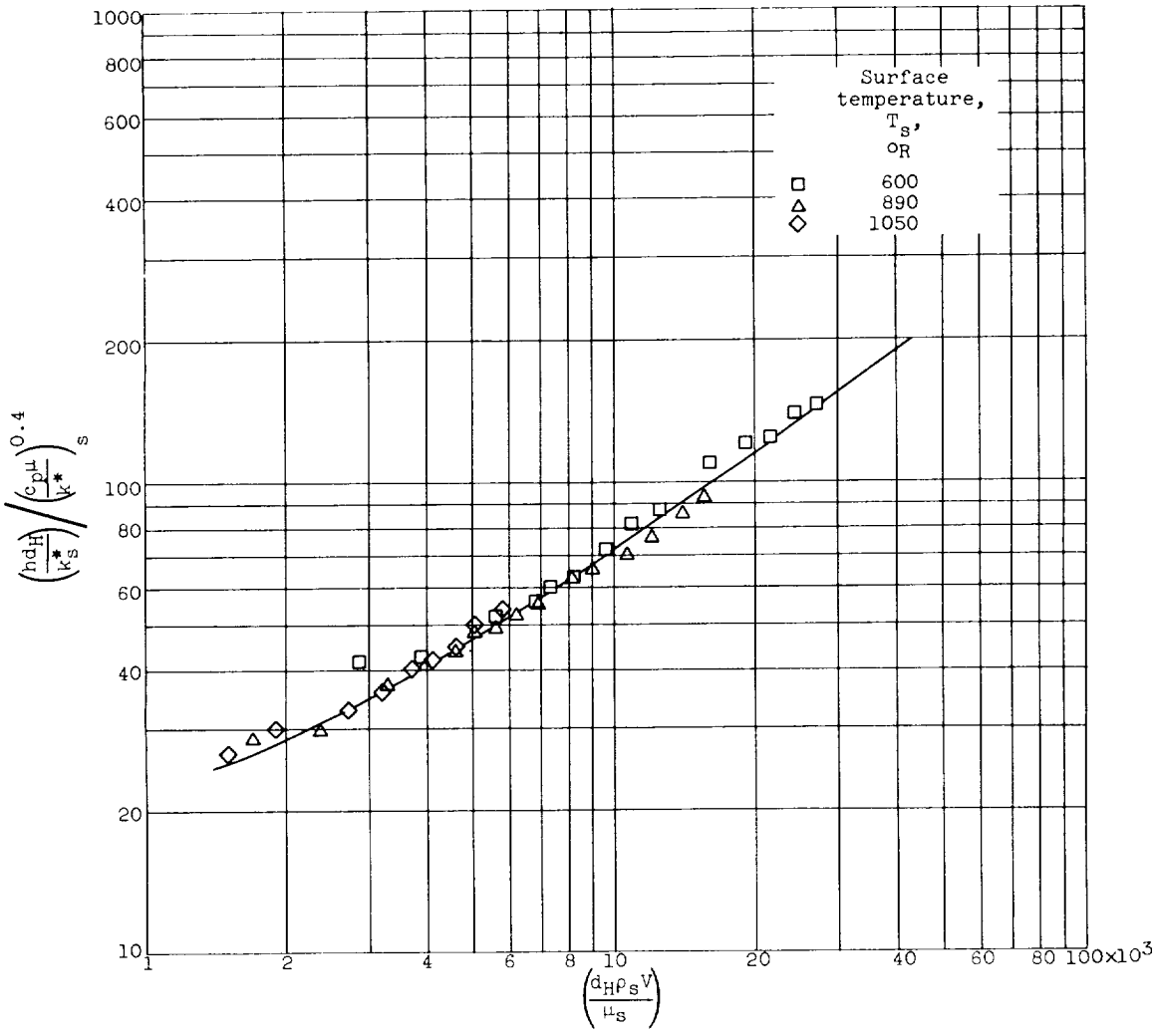

(d) Surface-density correlation, $k^* = 0.015\sqrt{T/530}$.

Figure 10. - Concluded. Heat-transfer and friction data for finned tubes.

NASA MEMO 10-9-58E
National Aeronautics and Space Administration.
HEAT-TRANSFER AND FRICTION MEASUREMENTS WITH VARIABLE PROPERTIES FOR AIRFLOW NORMAL TO FINNED AND UNFINNED TUBE BANKS.
Robert G. Ragsdale. December 1958. (i), 33p. diagrs., photos., tabs.
(NASA MEMORANDUM 10-9-58E)

Average heat-transfer and friction coefficients are reported for heat addition to air flowing normal to staggered banks of electrically heated finned and unfinned tubes for variable property conditions. The data are for Reynolds numbers from 2000 to 35,000 and surface-to-bulk temperature ratios from 1.07 to 2.36. The use of bulk density to evaluate Reynolds number is unsatisfactory. Single-line correlations are obtained by evaluation of specific heat, thermal conductivity, viscosity, and density at film and surface temperatures.

Copies obtainable from NASA, Washington

1. Heat Transfer, Aerodynamic (1.1.4.2)
2. Heat Transfer, Theory and Experiment (3.9.1)
3. Radiators (3.9.2.1)
I. Ragsdale, Robert G.
II. NASA MEMO 10-9-58E

NASA

NASA MEMO 10-9-58E
National Aeronautics and Space Administration.
HEAT-TRANSFER AND FRICTION MEASUREMENTS WITH VARIABLE PROPERTIES FOR AIRFLOW NORMAL TO FINNED AND UNFINNED TUBE BANKS.
Robert G. Ragsdale. December 1958. (i), 33p. diagrs., photos., tabs.
(NASA MEMORANDUM 10-9-58E)

Average heat-transfer and friction coefficients are reported for heat addition to air flowing normal to staggered banks of electrically heated finned and unfinned tubes for variable property conditions. The data are for Reynolds numbers from 2000 to 35,000 and surface-to-bulk temperature ratios from 1.07 to 2.36. The use of bulk density to evaluate Reynolds number is unsatisfactory. Single-line correlations are obtained by evaluation of specific heat, thermal conductivity, viscosity, and density at film and surface temperatures.

Copies obtainable from NASA, Washington

1. Heat Transfer, Aerodynamic (1.1.4.2)
2. Heat Transfer, Theory and Experiment (3.9.1)
3. Radiators (3.9.2.1)
I. Ragsdale, Robert G.
II. NASA MEMO 10-9-58E

NASA

NASA MEMO 10-9-58E
National Aeronautics and Space Administration.
HEAT-TRANSFER AND FRICTION MEASUREMENTS WITH VARIABLE PROPERTIES FOR AIRFLOW NORMAL TO FINNED AND UNFINNED TUBE BANKS.
Robert G. Ragsdale. December 1958. (i), 33p. diagrs., photos., tabs.
(NASA MEMORANDUM 10-9-58E)

Average heat-transfer and friction coefficients are reported for heat addition to air flowing normal to staggered banks of electrically heated finned and unfinned tubes for variable property conditions. The data are for Reynolds numbers from 2000 to 35,000 and surface-to-bulk temperature ratios from 1.07 to 2.36. The use of bulk density to evaluate Reynolds number is unsatisfactory. Single-line correlations are obtained by evaluation of specific heat, thermal conductivity, viscosity, and density at film and surface temperatures.

Copies obtainable from NASA, Washington

1. Heat Transfer, Aerodynamic (1.1.4.2)
2. Heat Transfer, Theory and Experiment (3.9.1)
3. Radiators (3.9.2.1)
I. Ragsdale, Robert G.
II. NASA MEMO 10-9-58E

NASA

NASA MEMO 10-9-58E
National Aeronautics and Space Administration.
HEAT-TRANSFER AND FRICTION MEASUREMENTS WITH VARIABLE PROPERTIES FOR AIRFLOW NORMAL TO FINNED AND UNFINNED TUBE BANKS.
Robert G. Ragsdale. December 1958. (i), 33p. diagrs., photos., tabs.
(NASA MEMORANDUM 10-9-58E)

Average heat-transfer and friction coefficients are reported for heat addition to air flowing normal to staggered banks of electrically heated finned and unfinned tubes for variable property conditions. The data are for Reynolds numbers from 2000 to 35,000 and surface-to-bulk temperature ratios from 1.07 to 2.36. The use of bulk density to evaluate Reynolds number is unsatisfactory. Single-line correlations are obtained by evaluation of specific heat, thermal conductivity, viscosity, and density at film and surface temperatures.

Copies obtainable from NASA, Washington

1. Heat Transfer, Aerodynamic (1.1.4.2)
2. Heat Transfer, Theory and Experiment (3.9.1)
3. Radiators (3.9.2.1)
I. Ragsdale, Robert G.
II. NASA MEMO 10-9-58E

NASA